applied sciences

MDPI

Article

Sewage Sludge Hydrochar: An Option for Removal of Methylene Blue from Wastewater

Roberta Ferrentino [1], Riccardo Ceccato [2], Valentina Marchetti [1], Gianni Andreottola [1] and Luca Fiori [1,*]

[1] Department of Civil, Environmental and Mechanical Engineering, University of Trento, via Mesiano 77, 38123 Trento, Italy; roberta.ferrentino@unitn.it (R.F.); marchetti.vale@libero.it (V.M.); gianni.andreottola@unitn.it (G.A.)

[2] Department of Industrial Engineering, University of Trento, via Sommarive 9, 38123 Trento, Italy; riccardo.ceccato@unitn.it

* Correspondence: luca.fiori@unitn.it; Tel.: +39-0461282692

Received: 20 April 2020; Accepted: 12 May 2020; Published: 16 May 2020

Featured Application: Producing a material—a product—from sewage sludge—a waste—resulting from wastewater treatment plants (WWTPs) is a possible sustainable solution to reduce the amount of sewage sludge to be disposed of. Thus, sewage sludge hydrochar (simply produced as detailed in the paper) having good adsorption capabilities could be used, for instance, in municipal and industrial WWTPs for water remediation.

Abstract: Municipal sewage sludge was subjected to a hydrothermal carbonization (HTC) process for developing a hydrochar with high adsorption capacity for water remediation in terms of dye removal. Three hydrochars were produced from municipal sewage sludge by performing HTC at 190, 220 and 250 °C, with a 3 h reaction time. Moreover, a portion of each hydrochar was subjected to a post-treatment with KOH in order to increase the adsorption capacity. Physicochemical properties of sludge samples, raw hydrochars and KOH-modified hydrochars were measured and batch adsorption studies were performed using methylene blue (MB) as a reference dye. Data revealed that both raw and modified hydrochars reached good MB removal efficiency for solutions with low MB concentrations; on the contrary, MB in high concentration solutions was efficiently removed only by modified hydrochars. Interestingly, the KOH treatment greatly improved the MB adsorption rate; the modified hydrochars were capable of capturing above 95% of the initial MB amount in less than 15 min. The physicochemical characterization indicates that alkali modification caused a change in the hydrochar surface making it more chemically homogeneous, which is particularly evident for the 250 °C hydrochar. Thus, the adsorption process can be regarded as a complex result of various phenomena, including physi- and chemi-sorption, acid–base and redox equilibria.

Keywords: hydrothermal carbonization; HTC; sewage sludge; hydrochar; methylene blue; adsorption; water remediation; value-added product; waste-to-products

1. Introduction

Sewage sludge is an unavoidable waste of municipal wastewater treatment activity. The production of sludge in municipal wastewater treatment plants (WWTPs) has increased due to more stringent legislation and a growing number of new plants, becoming a critical issue [1]. Several methods can be adopted for sludge management such as landfill disposal, incineration and, where possible and allowed by the legislation, utilization in agriculture. However, each of these options has important limitations [2]. This has prompted the search for more cost effective and environmentally

sustainable technologies able to promote the innovative and beneficial use of sewage sludge. Thus, the conversion of this class of waste products, as well as of organic wastes in general, into value-added products such as energy carriers, biomaterials, bioplastics and fertilizers is on the rise. A very appealing technology is hydrothermal carbonization (HTC) which, in recent years, has been proposed as a promising process that allows obtaining a solid carbonaceous material with different possible utilizations. This process is attractive due to its simplicity, low-cost and its energy and CO_2 containment efficiency. One of the major advantages of HTC over other technologies is its capability to convert wet biomass into solid products without the need for energy-intensive drying before and/or during the process [3], as HTC uses water as the reaction medium. High water content raw substrates such as animal manures, the organic fraction of municipal solid waste, sewage sludge, aqua culture and algal residues could be used as feedstock for the HTC process [4].

The HTC process is performed applying mild temperatures (180–260 °C) under saturated water vapor pressure for several hours [5,6]. Thus, the feedstock is subjected to a thermochemical process that includes simultaneous and sequential reactions of hydrolysis, dehydration, decarboxylation, condensation, polymerization and aromatization. However, the detailed reaction mechanisms are as yet unknown due to the complexity of the residual biomasses used as feedstock and the coexistence of several reactions in series and in parallel [7]. Reaction mechanisms involving complex biomasses can be investigated using a lumped components approach [8]. The resulting carbon rich solid product, referred to as hydrochar, is presently evaluated for use in a wide range of applications due to its properties and the diversity of materials used as feedstock. Proposed uses of hydrochar include its utilization as adsorbent material , carbon based smart material, energy vector and soil amendment [9]. Consequently, hydrochar is regarded as a valuable material for various industrial, environmental and agricultural applications. Regarding the use as an adsorbent material, hydrochar usually exhibits increased functional groups on its surface when compared with the raw biomass, which gives the hydrochar a high hydrophobicity, chemical affinity and potentialities towards adsorption applications [10,11]. For instance, Hammud et al. [12] performing HTC at 225 °C converted pine needles into hydrochar to remove malachite green dye from water and reached an adsorption capacity of 52.91 mg g^{-1}. Similarly, Wei et al. [13] used municipal sewage sludge as raw material to prepare an adsorbent by HTC (180 °C) and investigated its adsorption capacity for crystal violet. Results showed that the prepared hydrochar had a relatively high specific surface area, well-developed porosity and abundant surface organic functional groups that were beneficial for contaminant removal. Moreover, to enhance the adsorption capability of hydrochar, modification turned out to be an effective method [14]. By "modification" we mean a treatment in which the feedstock (hydrochar in this case) is treated with a chemical agent (e.g., KOH) via impregnation, which is not followed by a heat treatment at 500–850 °C in nitrogen typical of chemical activation [11,15–17]. For instance, Regmi et al. [18] tested the sorption capacities of KOH-modified hydrochar from switchgrass for removing copper and cadmium from aqueous solutions: they found a removal of about 100% within 24 h of contact time while the raw hydrochar only removed 16% of copper and 5.6% of cadmium. Similarly, Sun et al. [14] showed that alkali modification improved the sorption ability of hydrochars produced by HTC of sawdust, wheat straw and corn stalk. Moreover, Spataru et al. [19] tested a low-cost adsorbent derived from HTC of waste activated sludge after KOH treatment at room temperature for the removal of orthophosphate from the effluent of a municipal WWTP. The study demonstrated that modified hydrochar achieved more than 97% orthophosphate removal. Thus, literature studies demonstrate that the alkali modification process may positively affect hydrochar surface, thus improving its sorption capacity [14].

To date, no study has examined the adsorption capacity of municipal sewage sludge-derived hydrochar [13] compared to alkali modified hydrochar and, in addition, considering different HTC treatment temperatures. Thus, the aim of the present study is to investigate the adsorption capacity of sewage sludge hydrochar (raw or KOH-modified) obtained at different HTC operating conditions for dye removal from aqueous solutions using methylene blue (MB) as the adsorbate.

Importantly, these materials present some elements of complexity in comparison with other classes of organic-derived adsorbents: (i) the lower treatment temperatures give rise to products

displaying lower specific surface area values than activated carbon-based adsorbents, usually ranging from 800 to above 1100 $m^2 \cdot g^{-1}$; (ii) the presence in sewage sludges of alkaline and heavy metals cannot be neglected.

Thus, the feasibility of this application must take into account these two aspects: (1) the adsorption mechanism has to involve not only the surface morphology of the samples, but also some chemical reactions have to occur; (2) the presence of metal ions can provide acid–base or oxy-reductive processes with respect to the adsorbate: actually, MB is a positive-charged dye and it also displays reducing behavior in solutions (it can be used as an indicator in redox titrations).

With all these features in mind, the aim of this work is reached by performing the following main steps:

- preparation of three hydrochars from municipal sewage sludge by performing HTC at 190, 220 and 250 °C with a reaction time of 3 h;
- modification with KOH in order to increase the adsorption capacity of hydrochars;
- comparison of the physicochemical properties of raw and modified hydrochars using elemental analysis, thermogravimetry (TGA), nitrogen physisorption analysis, Fourier-transform infrared spectroscopy (FTIR), inductively coupled plasma spectroscopy (ICP) and flow injection mercury system (FIMS);
- comparison of the potential application of raw and modified hydrochars as adsorbents for MB removal by performing batch adsorption studies, namely adsorption isotherms and adsorption kinetics tests.

Even if the HCT of sewage sludge has been previously addressed by several authors, as far as we know, there are no studies performing such a detailed evaluation considering sewage sludge as feedstock for the HTC process and the derived hydrochar, possibly KOH-modified, as adsorbent material for MB removal. Therefore, the novelty of this study is on the investigation of the adsorption capacity of the derived hydrochars, the main adsorption mechanisms involved and the assessment of the best production conditions that enhance the adsorption capacity of sewage sludge hydrochars.

2. Materials and Methods

2.1. Materials

The sewage sludge, used as the feedstock, was a mixture of diluted sludge exiting the anaerobic digester (digestate), dry matter content 2.7%, and the same digestate downstream of the addition of polyelectrolyte and passage in centrifuge (palatable sludge), dry matter content 22%. The mixture was prepared in order to feed the HTC reactor with a stream sufficiently rich in dry matter content and, at the same time, where the biomass was completely submerged into a liquid phase: the resulting mixture had a dry matter content of 12%. The sludge mixture dry matter content was chosen to simulate the implementation in full-scale applications [20]. As a matter of fact, a sludge with a dry matter content equal to 12% can be easily pumped to the HTC reactor. Both digestate and palatable sludge were collected from the local WWTP of Trento North, Italy.

The preparation of MB solutions at different concentrations was conducted by adding the required amount of MB powder to deionized water. The activated carbon AquaSorb™ BP2, with a reported specific surface area of 900 $m^2 \cdot g^{-1}$, was also used to test the MB adsorption capacity so to compare the results obtained with those of the sewage sludge hydrochars and modified hydrochars.

2.2. Preparation and Modification of Hydrochar

HTC of sewage sludge was performed in a stainless steel AISI 316 batch reactor of 2 L internal volume. The reactor, built in house, was designed for temperatures and pressures, respectively, up to 300 °C and 140 bar. The reactor top flange is connected to two pipes that allow nitrogen gas purging in order to ensure not oxidizing conditions. The reactor is equipped with a pressure transmitter, two pressure gauges and four thermocouples positioned at different heights within it. The pressure and temperature transmitters send data to software that allows the control of the reactor temperature and

the monitoring of the four temperatures and the pressure. At the end of the HTC run, the reactor is cooled down to room temperature and then depressurized. Further details about the HTC reactor could be found in Merzari et al. [21].

1.7 kg of sewage sludge (0.8 kg of palatable sludge and 0.9 kg of digestate) were introduced into the reactor for each HTC run, in order to have a feedstock with a dry matter content equal to 12%. HTC tests were performed in duplicate at three different temperatures: 190, 220 and 250 °C, while the reaction time was set at 3 h for all the tests. At the end of each HTC run, the solid-phase material was separated from the liquid phase by vacuum filtration and later dried at 105 °C for 24 h to remove residual moisture. The obtained dry samples were designated as 190HC, 220HC and 250HC on the basis of their treatment temperature.

To produce the KOH-modified hydrochar, 5 g of hydrochar powder were mixed with 500 mL of a 2M KOH solution and then stirred for 1 h at room temperature. The modified hydrochars were separated from the liquid phase by vacuum filtration, then washed with deionized water and finally dried for 24 h at 105 °C. The obtained dry samples were labeled as 190MHC, 220MHC and 250MHC, on the basis of the treatment conditions as for the raw hydrochars, where M refers to the alkali modification process.

The hydrochar mass yield is here defined, as is the usual case [22], as the percentage ratio between the mass (on a dry basis, d.b.) of the solid (hydrochar) remaining after HTC and the mass (on a d.b.) of the raw sample before thermal treatment. Similarly, a mass yield is defined also for the KOH modification as the mass (on a d.b.) remaining after KOH treatment and the mass (on a d.b.) of the raw hydrochar before such treatment.

2.3. Materials Characterization

Elemental composition (carbon, C; hydrogen, H; and nitrogen, N) of the samples was assessed by using a LECO 628 analyzer (LECO, Moenchengladbach, Germany). Each analysis was performed in duplicate using about 0.1 g of sample per trial. Considering the ash value resulting from proximate analysis, the oxygen (O) content was calculated based on the mass difference [23].

In order to evaluate moisture (M), volatile matter (VM) and ash (A) contents of the samples, thermogravimetric analysis (TGA) was carried out by means of a Mettler Q5000 V3 (Columbus, OH, USA) thermobalance [24] and using about 30 mg of dried sample per trial. The thermal program, chosen from literature [25], can be considered as a modification of the ASTM reference methods E871, E872 and E830. To release residual moisture content, the sample was heated under air to 105 °C, temperature which was held for 30 min before heating at 16 °C/min from 105 to 900 °C (hold time: 7 min) in nitrogen to determine the volatile matter content. Ash was determined by switching to air while holding the temperature of 900 °C for an additional 30 min.

The surface morphological structure of the hydrochars was examined using a scanning electron microscopy (SEM) system (JEOL JSM-7001F Field Emission SEM, JEOL, Tokyo, Japan). The functional groups of the samples were examined by using Fourier transform infrared spectroscopy (FT-IR, Avatar 330, Nicolet, Waltham, MA, USA). Wavenumbers between 4000 and 400 cm^{-1} were covered using 64 scans in the investigation range with a resolution of 4 cm^{-1}. Moreover, the functional groups were examined using also FTIR-ATR (attenuated total reflectance) spectroscopy using a Spectrum One (Perkin Elmer, Boston, MA, USA) by averaging 16 scans with a resolution of 4 cm^{-1} in the wavenumber range between 4000 and 650 cm^{-1}, employing a ZnSe crystal. The load applied to squeeze the powdered samples towards the diamond was 130 ± 1 N.

The surface morphology and pore structure characteristics of the samples were determined by N_2 physisorption measurements performed at 77 K using a surface area porosimeter (ASAP 2010, Micromeritics, Norcross, GA, USA). All the samples were degassed below 1.3 Pa at 25 °C prior to the measurement.

The specific surface area was calculated following multipoint N_2-Brunauer–Emmett–Teller (BET) adsorption method, in the interval $0.05 \leq (P/P_o) \leq 0.33$. Pore size distribution curves were determined using the Brunauer–Joyner–Halenda (BJH) method applied both on the adsorption and the desorption branches of the isotherms.

The chemical speciation analysis of alkali and heavy metals and other elements undetectable by ultimate analysis was carried out in duplicate on raw sludges, hydrochars and modified hydrochars. Heavy metals concentrations were determined by using an optical ICP system (Perkin Elmer 7300 DV) and following UNI EN 13,657 and UNI EN ISO 11885:2009 methods. Mercury concentrations were determined by using a flow injection mercury system (FIMS) (Perkin Elmer FIMS 100). Total nitrogen concentrations were determined following CNR-IRSA Method [26].

2.4. Batch Adsorption Study

Adsorption isotherms of MB onto both raw and KOH-modified hydrochars were determined by adding 10–16 mg of absorbent to 25 mL stoppered glass bottles containing 4 mL of MB solution with various initial concentrations ranging between 10 and 300 mg L^{-1}. The bottles were agitated with a magnetic stirrer at 250 rpm and were kept at 20 ± 2 °C for 48 h. The pH of the MB solutions was evaluated using a portable pH meter (pH 3110 ProfiLine with SenTix41 probe, WTW, Milan, Italy). Then, the obtained solutions were centrifuged at 3000 rpm for 5 min and the MB concentrations were measured from the calibration curve of MB solutions at 665 nm using a UV-visible spectrophotometer (Model V-3250, Jasco Europe, Lecco, Italy). The adsorption capacity at equilibrium q_e (mg g^{-1}) and the percentage removal of MB were evaluated by Equations (1) and (2), respectively [27,28]:

$$q_e = (C_o - C_e)\ V/W \quad (1)$$

$$\%\ \text{removal} = ((C_o - C_e)/C_0)\ 100\% \quad (2)$$

where C_e and C_0 are, respectively, the equilibrium and initial MB concentration (mg L^{-1}), V is the solution volume (L) and W is the adsorbent mass used (g).

To investigate the mechanisms of adsorption, three well-known adsorption isotherms, Langmuir, Freundlich and Tempkin-type curves, were adopted. The Langmuir sorption isotherm is applied to equilibrium sorption assuming monolayer sorption on a surface with a finite number of identical sites. The linear Langmuir equation is expressed as Equation (3) [29]:

$$q_e = (K_L\ q_m\ C_e)/(1 + K_L\ C_e) \quad (3)$$

where K_L is the Langmuir constant (L mg^{-1}) related to the affinity of binding sites and the free energy of sorption, and q_m is the maximum adsorption capacity when a monolayer forms on the hydrochar (mg g^{-1}).

The Freundlich equation describes heterogeneous surface energy systems and is expressed as Equation (4) [30]:

$$q_e = K_F\ C_e^{(1/n)} \quad (4)$$

where K_F and 1/n are the Freundlich constants, determined from the plot of q_e versus C_e. The parameters K_F and 1/n are related to the sorption capacity and the sorption intensity of the system. The magnitude of the term 1/n gives an indication of the affinity of the sorbent/adsorbate systems [31].

The Tempkin equation is given by the following Equation (5) [32]:

$$q_e = B\ \ln\ (K\ C_e) \quad (5)$$

where B = (R T)/b, T is the absolute temperature in Kelvin, R is the universal gas constant (8.314 J mol^{-1} K^{-1}), b and K are Tempkin constants related to the heat of sorption (J mol^{-1}) and to the equilibrium binding (L g^{-1}), respectively.

The kinetics of MB adsorption on the raw and KOH-modified hydrochars were examined by adding 90 mg of each hydrochar to 150 mL glass bottles containing 50 mL of MB solution with a concentration of 100 mg L^{-1}. The glass bottles were then shaken at 250 rpm under a magnetic stirrer for 24 h. At different time intervals, the samples were centrifuged at 3000 rpm for 5 min and the residual MB concentration was measured by the UV-visible spectrophotometer (Model V-3250, Jasco Europe, Lecco, Italy) through the calibration curve.

The kinetics of the MB adsorption process was evaluated using pseudo-first order and pseudo-second-order kinetic models. The kinetic equations for these models are expressed by Equations (6) [33] and (7) [34], respectively:

$$\ln(q_e - q_t) = \ln q_e - k_1 t \quad (6)$$

$$t/q_t = t/q_e + 1/(k_2 q_e^2) \quad (7)$$

where q_e (mg g^{-1}) and q_t (mg g^{-1}) denote the MB sorption at equilibrium and time t (min), respectively, and k_1 (min^{-1}) and k_2 (g mg^{-1} min^{-1}) represent, respectively, the pseudo-first and pseudo-second order adsorption rate constants.

3. Results and Discussion

3.1. Characterization

Mass yields, elemental and proximate compositions and specific surface area of the various samples are reported in Table 1. Results reveal that the mass yield and the C content of the raw hydrochars are consistent with literature studies [35]. There was a significant decrease in mass yield at increasing HTC reaction temperature: when the reaction temperature rose from 190 to 250 °C, the hydrochar yield dropped down from about 83% to 63% and the C percentage increased from 26.9% to 36.3%.

Table 1. Mass yields, main physicochemical characteristics and elemental and proximate compositions of all the samples.

Samples	Mass Yield [%]	Elemental Composition (wt%, db)				Ash [%]	VM [% db]	FC [% db]	Atomic Ratio		Surface Area [m^2 g^{-1}]
		C [%]	H [%]	N [%]	O [1] [%]				H/C	O/C	
Digestate	-	25.6	4.0	3.6	21.9	45.0	50.2	4.8	1.88	0.64	-
Palatable	-	35.9	5.4	5.8	24.4	28.4	65.6	5.9	1.81	0.51	-
Mixture	-	34.4 [2]	5.2 [2]	5.5 [2]	24.1	30.8	63.4	5.7	1.81	0.53	-
190HC	83.3	26.9	5.1	3.0	20.5	44.5	55.2	0.3	2.28	0.57	31.00
220HC	76.3	28.2	4.0	1.8	18.5	47.5	52.4	0.1	1.70	0.49	8.82
250HC	62.9	36.3	5.0	5.0	8.7	45.0	54.9	0.1	1.65	0.17	11.85
190MHC	51.5	29.4	4.1	1.9	15.8	48.8	51.1	0.1	1.67	0.40	0.29
220MHC	71.2	33.6	4.4	3.0	9.5	49.5	50.0	0.5	1.57	0.20	2.74
250MHC	84.7	30.6	4.0	2.1	11.2	52.1	45.3	2.6	1.57	0.27	13.36

[1] oxygen content is estimated as follows: O = 100 − (C+H+N+ash). [2] calculated as the average of the values of digestate and palatable (weighted average considering the relevant dry matter content) the absolute errors for mass yield are ≤ ±2.4, the absolute errors for C, H, N are, respectively, ≤ ±1.0, ±0.2, ±0.3.

The KOH treatment reduced the mass of the hydrochar with a clear trend: the higher the temperature at which the hydrochar was produced, the higher the KOH treatment yield. This behavior is in agreement with previous results obtained coupling HTC with classical KOH chemical activation [11] and testifies the higher stability of hydrochars obtained at higher temperatures.

Considering the elemental composition (H, C, N, O), the O percentage is maximal for the three raw sludges and decreases with the HTC reaction temperature, as expected. Interestingly, the KOH treatment significantly reduced the O content in the samples obtained at 190 and 220 °C. Once more, this testifies the higher stability of hydrochars obtained at higher temperatures. The reduction in O can be due to the loss of volatile matters comprising some surface functional groups containing O [35].

Conversely, results related to the content of N and H do not show a clear trend in both raw and modified hydrochars.

The carbon content data are particularly interesting and testify to the peculiarity of this type of substrate, which behaves differently than the more standard biomass (e.g., agro-industrial biowaste,

ligno-cellulosic biomass, organic fraction of municipal solid waste). If for standard biomasses the HTC leads to an increase in the C percentage in the solid, here, on the contrary, the C percentage in some cases even decreased, passing for example from the value of 34.4% in the sludge mixture to the value of 26.9% in the hydrochar obtained at 190 °C. This atypical trend is explained by the remarkable ash content that characterizes the sewage sludge. HTC actually concentrates the ashes which, for the two samples mentioned above, passed from the value of 30.8% to the value of 44.5%. For sewage sludge, the C concentration effect is observable if the percentage values are considered on a dry ash free (daf) basis, less observable or not observable at all if the percentage values are considered on a dry basis. Thus, on a daf basis, the sludge mixture and the hydrochar obtained at 190 °C had a comparable carbon content (about 49%), and the carbon content rose for all the other hydrochars, both raw and KOH-modified, and it was in the range of 54%–67%. Therefore, for these types of substrate, the carbon enrichment takes place at the net of their ash content: the concentration effect of minerals masks the carbon concentration effect which is typical of HTC.

Regarding proximate analysis data, the ash content shows a significant increase after HTC, as expected. Moreover, a further increase is observed for the alkali-modified samples: among all the samples, the highest ash content (about 52%) was measured for the 250MHC.

The volatile matter of the sludge mixture reduced from about 63% to 52%–55% with the carbonization treatment, justifying the corresponding increase in mineral ashes [36]. Results show that there is no a significant difference in the VM content of the three raw hydrochars. Furthermore, the KOH treatment reduced even more the VM content of the hydrochars, which resulted in a range from about 51% (190MHC) to 45% (250MHC). Accordingly, the ash content after the KOH treatment increased up to 52% (250MHC). However, the decrease in VM was not accompanied by an increase in fixed carbon content. This indicates that VM was also converted into other products, such as CO_2 or liquids [37,38]. Despite the reported data of FC content, which honestly appears quite controversial (actually, in the general case HTC increases FC, which is not the case here), the same thermogravimetric analysis testifies that both raw hydrochar and modified hydrochar samples show an increased thermal stability if compared to raw sludge samples, as expected. This is clear when considering the derivative thermogravimetric (DTG) curves in N_2: Figure A1 in Appendix A. The temperature at which the decomposition rate was maximal was around 280 °C for digestate, palatable and mixture sludge, while it was in the range 450–480 °C for raw and modified hydrochars.

Considering H/C and O/C atomic ratios, general trends appear even if some data are out of trend, likely due to the heterogeneity of this kind of substrates. H/C and O/C atomic ratios decreased after HTC, and they decreased even more after KOH post-treatment. The higher the temperature of the HTC process, the lower are the H/C and O/C ratios. Thus, increasing the reaction severity resulted in a decrease of H/C and O/C ratios.

The BET specific surface area values of hydrochars were 31.00, 8.82 and 11.85 $m^2\ g^{-1}$ for 190HC, 220HC and 250HC, respectively. Thus, sample 190HC had the highest surface area value. However, after treatment with KOH, samples 190 MHC and 220MHC showed very low BET surface areas in comparison with raw hydrochars, accounting for 0.29 and 2.74 $m^2\ g^{-1}$ respectively. Similar results and trends were observed also for cold alkali modification of other hydrochars as reported in previous studies [10,14,28]. A low apparent BET surface area can be related to pore blockage due to organic compounds that were not transferred to the liquid phase during KOH treatment [10]. On the contrary, the BET surface area of sample 250MHC slightly increased after the treatment with KOH reaching the value of 13.36 $m^2\ g^{-1}$.

Figure 1 shows adsorption/desorption branches for nitrogen isotherms at 77 K of raw (Figure 1a) and modified (Figure 1b) hydrochars. The desorption branch of sample 190MHC is not reported because it is superimposed onto the adsorption one, due to the low BET surface area value. All hydrochars present gas physisorption isotherms of type II b according to the IUPAC classification [39], typical of materials with slit macro-pores with an average diameter of around 100 nm and attributable to the formation of aggregates of discoidal particles. Macro-pores were present in small amount in all samples, thus confirming the low values of BET surface area observed. Adsorption/desorption isotherms are very close, indicating a narrow and homogenous pore

distribution. Moreover, the presence of the hysteresis loop confirms the prevalent presence of macropores, except for the 190MHC sample. Furthermore, the shape of the hysteresis loop is of type H3, located at the high relative pressure range, displaying two steep, parallel branches, without a plateau. This shape indicates the presence of flat particles and slit pores. After the KOH treatment, hysteresis loops are wider, especially for the sample 220MHC, due to an amplification of the pore distribution curve. Moreover, in the case of sample 220MHC the shape of the hysteresis loop can be considered as intermediate between type H3 and H4, indicating a higher reduction in the number of pores compared to the other modified hydrochars. As expected, specific surface area values are much lower in comparison with reported ones for activated carbon materials, obtained from different organic sources [40,41]. However, the presence of various functional groups on the sample surfaces, the alkaline treatment and the presence of metal ions could modify in a more efficient way the interactions between adsorbent and MB adsorbate, as already reported for low-temperature treated organic-based adsorbents [42]. SEM micrographs (Figure A2 in Appendix A) show a smooth surface without pores in the micrometer size range for all the samples investigated.

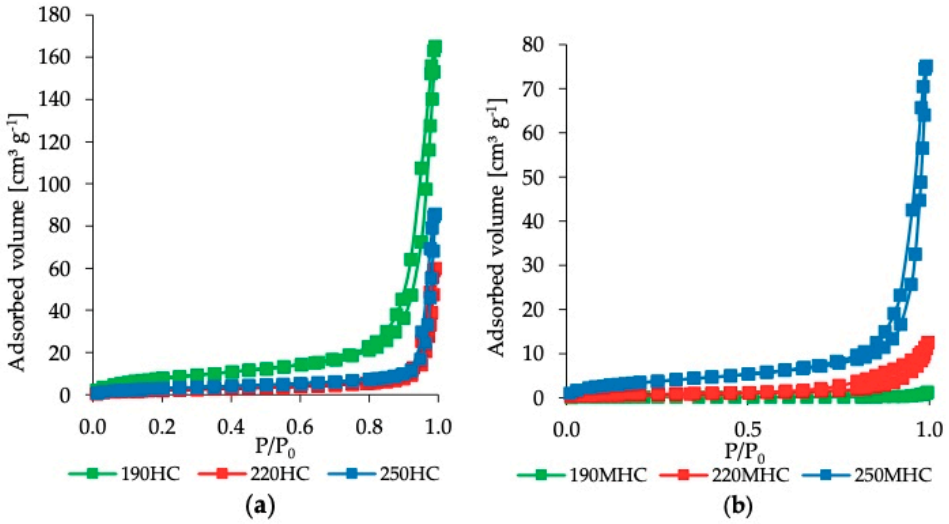

Figure 1. Nitrogen adsorption/desorption isotherms at 77 K of (**a**) raw and (**b**) modified hydrochars.

The FTIR analysis results of raw and modified hydrochars are illustrated in Figure 2. This analysis allows determining of the main functional groups present on the hydrochars' structures, which could attribute to them different adsorption capacities. The FTIR spectra of raw (Figure 2a) and modified (Figure 2b) hydrochars are quite similar in terms of their functional groups, since peaks fall in the same wavenumber interval. The bands within the range of 3600–3000 cm^{-1} correspond to O–H groups such as alcohols, phenols and carboxylic acids. These groups can provide hydrochars with good cation exchange capacity [6,43], just like MB, that is positively charged. Moreover, the peak has a fairly wide width meaning that there is a complex interaction among the same surrounding functional groups. The bands at 2920–2850 cm^{-1} are attributable to aliphatic C–H stretching bonds, as due to -CH_2 (methylene) or -CH_3 (methyl) groups, without aromatic components. The bands within the range of 1650–1530 cm^{-1} could correspond to C–O groups of amide groups and carboxylates. From a qualitative point of view, samples obtained at 190 °C do not show enhanced structural changes before and after the basic treatment, unless a decrease in intensity of the band located at about 1630 cm^{-1}, maybe due to a decrease in the adsorbed water content. For the samples produced at higher temperatures, a general decrease in intensity for the signals related to oxygen-containing functional groups was observed with the alkaline treatment, as a result of the partial removal of these groups from the sample surfaces, leading to a more homogeneous outer structure, as also evidenced by SEM analysis, confirming data from the elemental analysis.

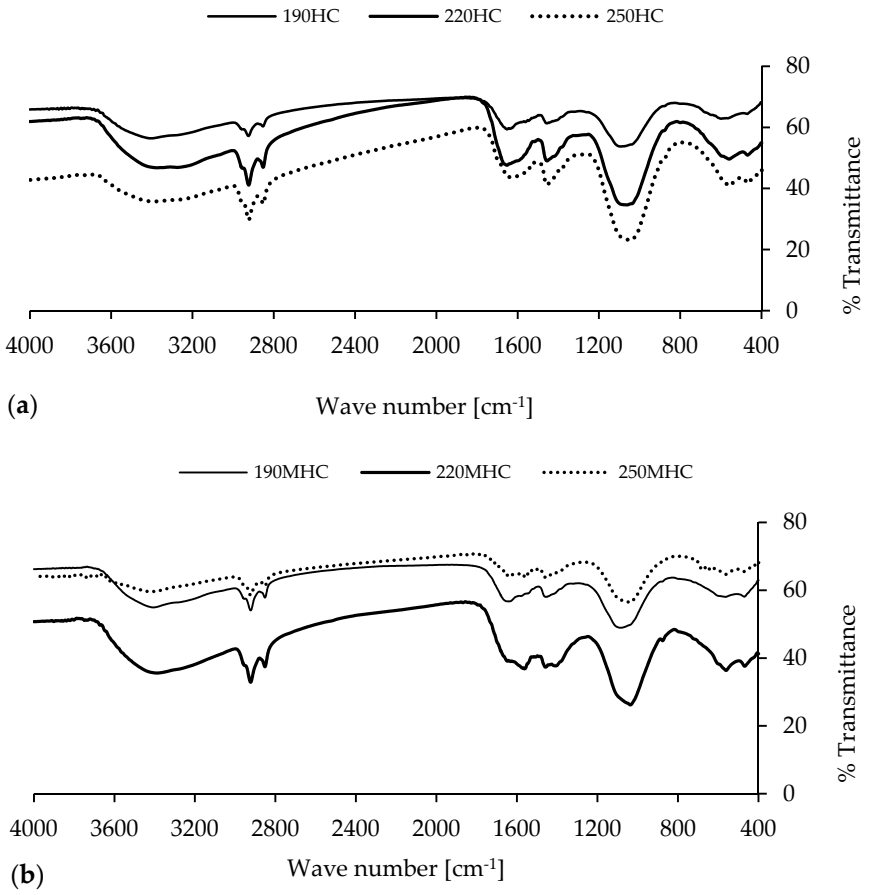

Figure 2. Fourier transform infrared spectroscopy (FTIR) spectra of (**a**) raw and (**b**) modified hydrochars.

The HTC treatment has a significant effect on the amount of heavy metals in the sewage sludge hydrochars [44]. The total contents of heavy metals, alkali earth metals and nutrient elements in the various samples is presented in Figure 3. In Table A1 in Appendix A the concentration values are reported. As evident from Figure 3, considerable amounts of N, Ca, Fe and P were present in the raw sludge mixture, followed by Al, Mg and K. Cu, Na and Zn were present in lower concentration. Cd, Cr, Ni, Hg and Pb are not reported in Figure 3 as their concentration is lower than 30 mg kg^{-1}. Since heavy metals mostly remain in the solid phase after HTC treatment, their concentration in the hydrochars increased [45] with the formation of more adsorption points to adsorb heavy metal ions [46]. Considering alkali metals, the HTC treatment concentrated both Ca and Mg in the hydrochar, while Na and K concentration decreased due to their solubility (and thus partial dissolution) into the HTC process water [47]. The KOH treatment did not substantially vary the concentration of metals in the hydrochars with some exceptions: the Mg and Na concentrations slightly increased while the increase in K concentration was extremely high. As a matter of fact, some K deriving from the KOH used to modify the hydrochars remained in the hydrochars themselves. The presence of metal ions with basic properties (K, Ca, Al) can improve the efficiency of acid–base interactions with MB, displaying acid behavior, thus an improvement of MB removal is expected in more basic environments [42]. Moreover, it should not be neglected that the presence of Fe ions in raw and modified hydrochars could improve the MB removal efficiency, due to the onset of a redox equilibrium between Fe ions and MB itself.

Furthermore, our data also prove that the HTC of sewage sludge is a process which enriches the resulting solids in P [48]. The produced hydrochar has thus a higher concentration of P compared to the raw sludge mixture; P which, together with other elements such as N, K, Na, Ca and Mg, is an essential nutrient for plants growth.

It is worthy commenting on the N content data calculated via ICP with that calculated via CHN analysis through the elemental analyzer. The data for the sludge mixture is statistically identical (ICP: 5.3% ± 0.1%; CHN analysis: 5.5% ± 0.3%). When considering raw and modified hydrochars, such data consistency is found only for three samples out of six: for three hydrochars, the values measured by the two techniques are statistically different. This could be due to some extent to the different analytical approach but, in the opinion of the authors, this is mainly due to the natural heterogeneity of the samples, also considering that each sample derives from the mixing of two different sludges having different chemical characteristics.

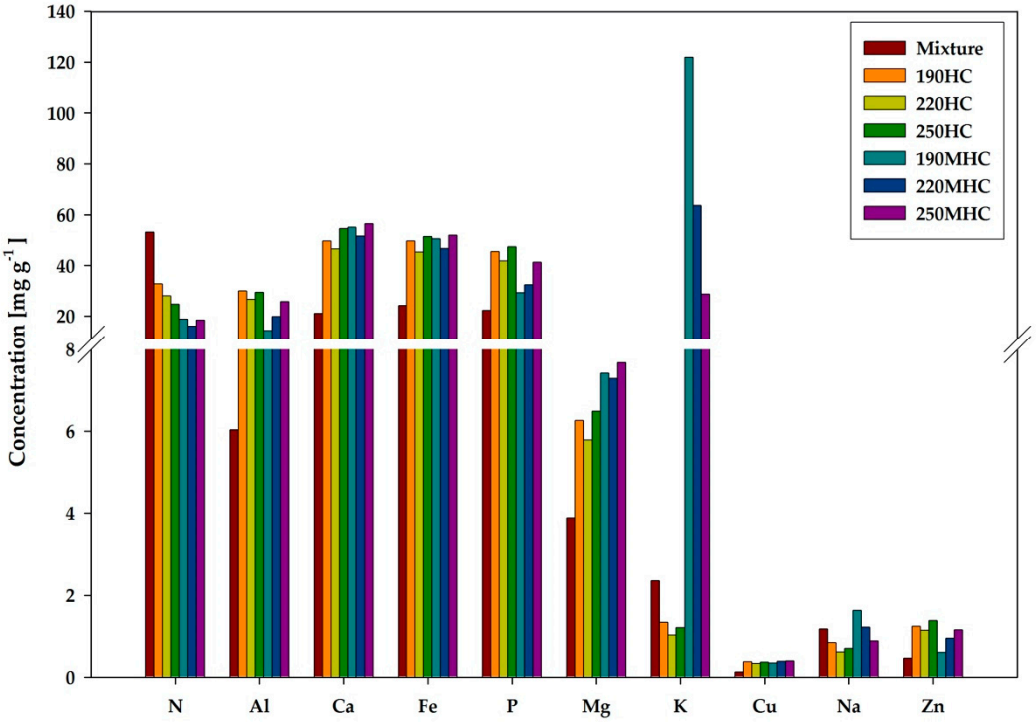

Figure 3. Heavy metals, alkali metals and nutrient content in mixture sludge, raw and modified hydrochars.

3.2. *Adsorption Isotherms*

The equilibrium adsorption isotherm is studied in detail, since it can provide information about the surface properties of hydrochars and their adsorption behavior. Adsorption equilibrium is a dynamic concept, i.e., it is achieved when the rate of (dye) adsorption is equal to the rate of (dye) desorption [49].

Figure 4 depicts the MB adsorption isotherms onto raw hydrochars, modified hydrochars and activated carbons.

Considering raw hydrochars (Figure 4a), isotherms are of the same type; they are characterized by a large increase in the amount adsorbed at low concentrations, while the amount adsorbed stabilizes around a limit value, different for the various hydrochars, when the concentration is higher. For all the treatment temperatures the q_e increased quickly for C_e lower than 30 mg L^{-1}, while the increase in q_e slowed down for C_e values higher than 50 mg L^{-1}. The amount of adsorbed MB increased when the HTC treatment temperature increased from 190 to 220 °C; on the contrary, the amount of adsorbed MB decreased for the hydrochar obtained at 250 °C. However, the hydrochar that revealed the best adsorption capacity is the 190HC because it shows the lower C_e concentration (95 mg L^{-1}) compared to samples 220HC (150 mg L^{-1}) and 250HC (190 mg L^{-1}), when the equilibrium is reached using the most concentrated initial MB solution (295 mg L^{-1}). These findings, which may

appear to be contradictory, are explained by the fact that the quantity of hydrochar used in the various tests was slightly variable (Section 2.4 and Tables A2 and A3 in Appendix A).

The q_e increased quickly for low values of C_e for modified hydrochars (Figure 4b), too. However, the isotherm trends are quite different from those of raw hydrochars. Thus, it is clear that the KOH treatment produced strong changes in the adsorption characteristics of the hydrochars. Actually, for all the modified hydrochars the C_e values, measured after 48 h of test, are much lower (maximum C_e value: 30 mg L^{-1}) than those of raw hydrochars (maximum C_e value: 190 mg L^{-1}) and this corresponds to a higher amount of MB adsorbed. Considering all the hydrochars, the sample that shows the best adsorption capacity is 250MHC, i.e., that produced by HTC of sewage sludge at 250 °C for 3 h and post-treatment with KOH. In Figure 4b the adsorption isotherm trend for activated carbons is depicted, too. As expected, the q_e increased very quickly, reaching a value of 113 mg g^{-1} at the highest C_0 concentration, and C_e values were very reduced and always lower than 0.65 mg L^{-1}.

The pH values of the MB solutions were evaluated. The pH value slightly increased after the addition of MB to the deionized water, passing from a value of 5.5, referring to the deionized water, to values in the range 6.2–6.6. The trend of the pH variation corresponding to a MB concentration ranging between 10 and 300 mg L^{-1} has been reported in Figure A3 in Appendix A.

The percentages of MB removed by hydrochars, referring to different C_0 of the MB solutions, are reported in Figure 5.

Figure 5a shows the MB removal of raw hydrochars. Results reveal a high MB removal efficiency for initial concentrations of MB ranging between 10 and 100 mg L^{-1} accounting for an average value of 90%, 95% and 87% for samples 190HC, 220HC and 250HC, respectively. The removal efficiency decreased below 87% (190HC), 89% (220HC) and 65% (250HC) for C_0 values higher than 150 mg L^{-1}.

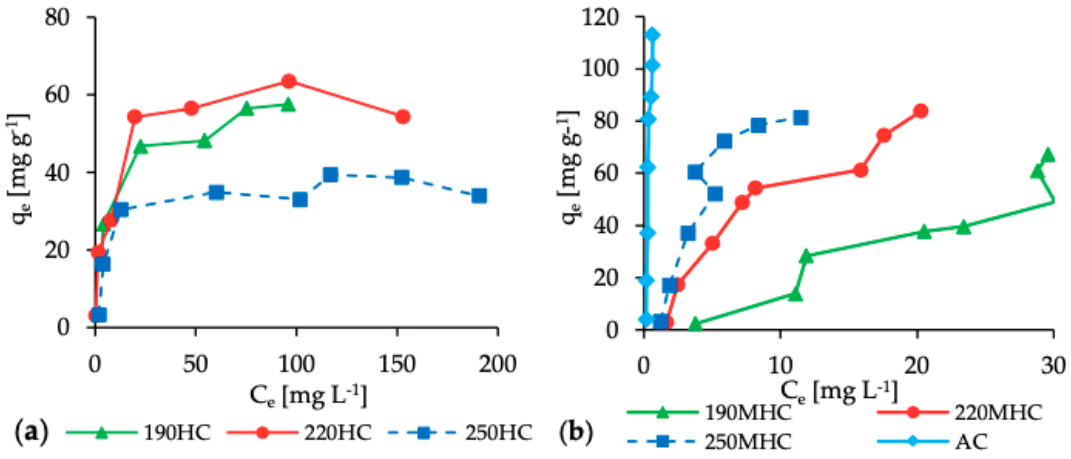

Figure 4. Methylene blue (MB) adsorption isotherms on (**a**) raw hydrochars and (**b**) modified hydrochars and activated carbons, AC.

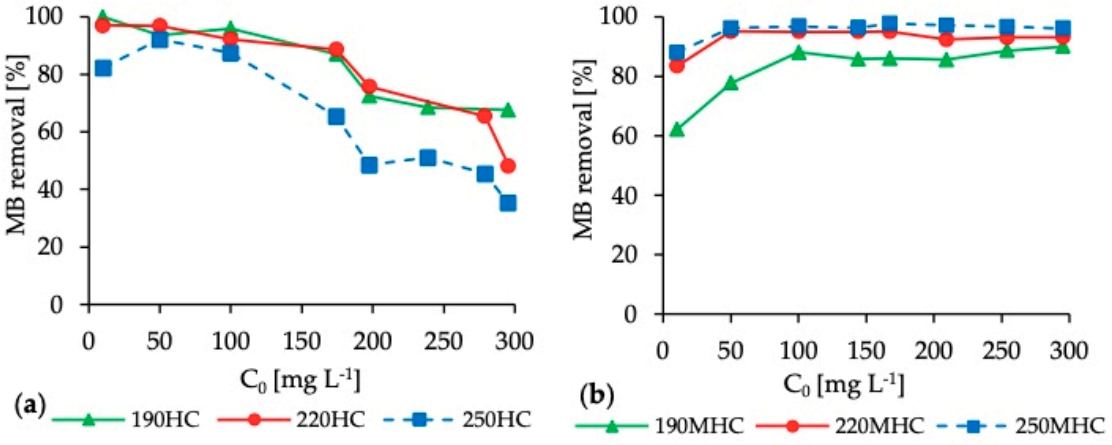

Figure 5. MB removal percentage corresponding to different C_0 values of MB solutions by (**a**) raw hydrochars and (**b**) modified hydrochars. Removal efficiency by activated carbons was always greater than 99% and thus not reported.

However, the reduction in MB removal efficiency was slow for samples 190HC and 220HC reaching 68% and 48%, respectively, for C_0 equal to 300 mg L^{-1}, while sample 250HC showed a quite quick reduction in the MB removal efficiency accounting for 48% already in correspondence of a C_0 value of 200 mg L^{-1} and further, to 35% for a C_0 equal to 300 mg L^{-1}. Considering the KOH modified hydrochars (Figure 5b), results show an increasing MB removal efficiency for initial concentrations of the MB solutions ranging between 10 and 100 mg L^{-1} accounting for 88%, 95% and 97% for sample 190MHC, 220MHC and 250MHC, respectively, at C_0 equal to 100 mg L^{-1}. Further, these removal efficiencies remained stable for C_0 values up to 300 mg L^{-1} confirming that the treatment with KOH caused a significant change in the structure of the hydrochars produced at all the HTC temperatures investigated and enhanced the adsorption capacity for removing MB from the aqueous solutions.

As expected, results of the MB adsorption isotherms onto activated carbon revealed a high MB removal efficiency (≥99%) for all the initial concentrations of MB investigated. The equilibrium adsorption data were analyzed using Langmuir, Freundlich and Tempkin adsorption isotherm models. The linear MB adsorption plots for raw and modified hydrochars by the three models are shown in Figure A4 in Appendix A.

Table 2 summarizes the parameters of Langmuir, Freundlich and Tempkin isotherms and the correlation coefficients; the parameters were obtained from the intercepts and slopes of the straight lines resulting from the linear regression of the data points.

Table 2. Parameters used in Langmuir, Freundlich and Tempkin equations.

Samples	Langmuir Equation			Freundlich Equation			Tempkin Equation		
	q_m (mg g^{-1})	K_L (L mg^{-1})	R^2	K_F (L mg^{-1})	n	R^2	B	K (L g^{-1})	R^2
190HC	70.51	0.05	0.9923	5.78	5.81	0.9151	12.49	1.20	0.9589
220HC	54.29	0.38	0.9676	9.74	2.44	0.7733	8.78	6.12	0.7122
250HC	37.64	0.14	0.9845	5.83	2.52	0.7659	6.43	2.57	0.7801
190MHC	247.06	0.01	0.1237	3.60	1.24	0.8000	34.51	0.17	0.8201
220MHC	140.13	0.06	0.8694	10.74	1.45	0.9412	29.35	0.70	0.9525
250MHC	203.16	0.07	0.4208	13.89	1.21	0.8156	36.36	0.98	0.8823

For raw hydrochars, results show that the correlation coefficients for Langmuir isotherms are significantly higher than those for Freundlich and Tempkin isotherms. The Langmuir isotherms describe closely the MB adsorption by raw hydrochars, suggesting that adsorption is localized on a

monolayer and all the adsorption sites are homogeneous [50]. The maximum value of adsorption capacity is 70.51 mg g^{-1}, related to the sample subjected to 190 °C HTC process. After the treatment with KOH of this sample, the adsorption capacity increased to 247.06 mg g^{-1} according to the linear regression. However, after KOH treatment the correlation coefficient decreases strongly for the 190 °C samples (from 0.9923 to 0.1237), and this behavior is also observed for the 220 and 250 °C samples, meaning that the modified hydrochars do not follow Langmuir isotherms. On the contrary, Tempkin isotherms exhibit higher correlation coefficients for MB sorption by the modified hydrochars indicating the physicochemical nature of the sorption process with a multilayer coverage of active sites on the adsorbent surface [51]. Results show an R^2 equal to 0.8201, 0.9525 and 0.8823 for samples 190MHC, 220MHC and 250MHC, respectively. The equilibrium data were also fitted to the Freundlich equation. Data show good correlation coefficients, in particular for the modified hydrochars; however, they were lower than Langmuir (for HC) and Tempkin (for MHC) values meaning that the MB adsorption does not follow Freundlich model closely.

3.3. Adsorption Kinetics

Kinetics data for the adsorption of MB onto both the raw and modified hydrochars versus contact time are presented in Figure 6a and b, respectively.

Sorption of MB onto HC (Figure 6a) increased rapidly during the initial 2 and 4 h of contact time for 190HC and 220HC, respectively. For both samples, sorption increased a little more until 6 h of contact time and then slowly, reaching an asymptotic value: 41.8 mg g^{-1} and 41.2 mg g^{-1} for 190HC and 220HC, respectively. The trend for sample 250HC differs significantly from those discussed above. The adsorption of MB onto sample 250HC occurs very slowly with a q_t that increases from 10.2 to 29.4 mg g^{-1} during 8 h of contact time, finally reaching a value of 37.5 mg g^{-1} at 24 h. Thus, this observation is consistent with the adsorption isotherm results, where sample 250HC showed a lower adsorption capacity compared to samples 190HC and 220HC.

Considering the modified hydrochars (Figure 6b), the adsorption of MB onto MHC increased very rapidly. Samples 190MHC and 220MHC reached both a q_t value equal to 48.0 mg g^{-1} after only 15 min of contact time and this value remained quite stable up to 24 h. Sample 250MHC shows an adsorption of MB slightly slower than the other two samples; the q_t value increased up to 50 mg g^{-1} during the initial 2 h of contact time and then remained stable until 24 h. Thus, at the maximum contact time tested all the samples show approximately the same adsorption capacity accounting for 50.0, 52.5 and 51.5 mg g^{-1} for 190MHC, 220MHC and 250MHC, respectively. It is evident that the KOH-treated hydrochars reach a higher value of q_t compared to the raw hydrochars. The adsorption of MB onto MHC, especially for samples 220MHC and 250MHC, is to some extent comparable to that of the activated carbon. In all cases, the adsorption of MB was very rapid. Moreover, the adsorption capacity of the activated carbon resulted equal to 64.3 mg g^{-1}, that is about 22% higher than that of the MHC samples.

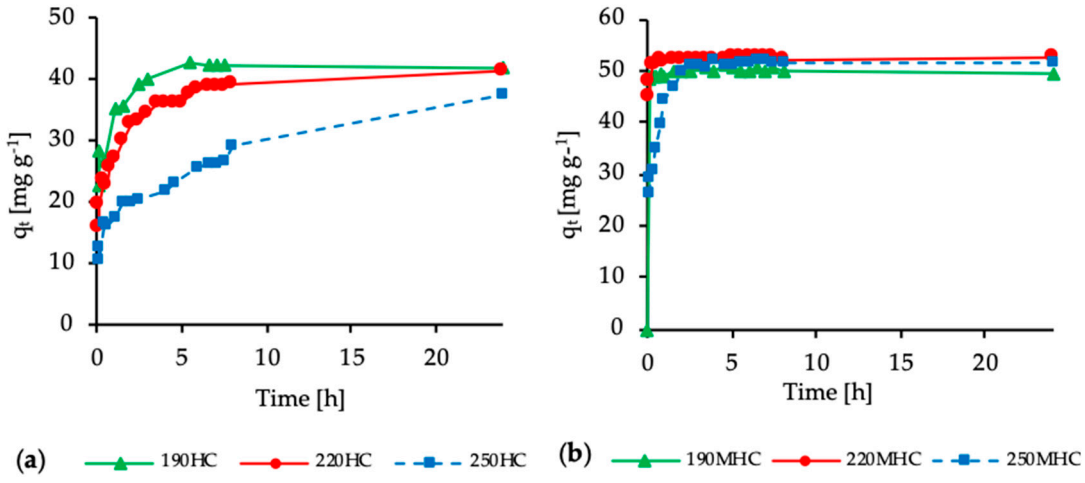

Figure 6. MB adsorption kinetics on (**a**) raw and (**b**) modified hydrochars.

The trends of 190HC, 220HC, 190MHC, 220MHC and 250MHC are similar; in all the samples the sorption of MB onto hydrochars increased during the first period of contact time and then slowed down significantly until an asymptotic value was reached, most probably related to an equilibrium stage. This can be explained considering that there are available active sites on the adsorbent that are reduced gradually with the adsorption progress [28]. The main difference between raw and modified hydrochars is the adsorption rate; what happens for the raw hydrochars within 8 h of contact time occurs, instead, for the modified hydrochars within 15 min or at most 2 h. This means that the treatment with KOH causes a change in the hydrochar structure and surface, speeding up the adsorption process.

The pseudo-first order and pseudo-second order kinetic models were used to evaluate the kinetics of the MB adsorption process. Data and related linear regression lines for the two models are reported in Figure A5 (see Appendix A) while Table 3 reports the calculated kinetics parameters.

Table 3. Kinetics parameters for the adsorption of MB onto raw and modified hydrochars.

Sample	Pseudo First-Order			Pseudo Second-Order		
	q_e (mg g^{-1})	k_1 (min^{-1})	R^2	q_e (mg g^{-1})	k_2 (g mg^{-1} min^{-1})	R^2
190HC	22.46	0.0125	0.8897	42.15	0.0041	0.9997
220HC	21.18	0.0053	0.9378	41.56	0.0008	0.9990
250HC	24.94	0.0021	0.8783	36.65	0.0003	0.9631
190MHC	4.79	0.0390	0.3351	49.54	−0.0080	0.9999
220MHC	13.03	0.0740	0.7815	52.56	0.0190	0.9999
250MHC	37.95	0.0310	0.9501	52.01	0.0030	0.9998

The correlation coefficients of the second order kinetic model are greater and closer to unity ($R^2 > 0.95$) than those of the first order kinetic model for both the raw and modified hydrochars obtained at all the HTC treatment temperatures. These results reveal that the pseudo second-order equation is preferable to describe the adsorption kinetics, and it is very accurate for five samples ($R^2 \geq 0.999$) out of six. Thus, the adsorption process involved chemical interactions between MB and the polar functional groups present at the surface of HC and MHC [34].

3.4. Effect of KOH Modification

As reported above, differences between raw and modified hydrochars are notable for all the HTC treatment temperatures. In general, the KOH treatment significantly enhanced the adsorption capacity of MB onto hydrochars, showing also that MB in high concentrations in the range of 200–300 mg L^{-1} could be easily adsorbed. These results are consistent with the FTIR analysis which has shown that the KOH treatment causes a change in the hydrochar surface making it more homogeneous, which contributes significantly to an increase in the adsorption capacity of the modified hydrochars. However, the KOH treatment does not have the same effect on all of the hydrochars. In particular, the alkali modification on the 250MHC sample provided a sort of "soft cleaning effect" on the hydrochar surface, as reported by SEM analysis, which is consistent with the slight increase in the surface area proved by the BET model. This means an increased number of surface active sites available for the adsorption corresponding to an increase in the MB adsorption capacity of MHCs. Conversely, the KOH treatment applied at hydrochars obtained at the lower temperatures was detrimental in terms of surface area, which dramatically decreased for the hydrochar obtained at 190 °C, passing from 31 for the raw hydrochar to 0.29 m^2 $g^{-1}$for the KOH-treated sample—a similar but less pronounced effect was observed for the 220 °C hydrochars. Considering adsorption tests, consistently the 190MHC performed the worst when compared to the other MHCs.

Conclusively, results reveal that the alkali treatment on hydrochars generates different effects depending on the HTC treatment temperature, to which different hydrochars characteristics and chemical stability correspond. A common feature is that for all the hydrochars, the KOH post-treatment increased the MB adsorption rate and, more generally, increased their performances as adsorbents.

4. Conclusions

Sewage sludge hydrochars were tested as adsorbents as such and after a KOH post-treatment step. Results indicate that both raw and alkali-modified hydrochars could be used as adsorbents for MB solutions and, more in general, for the treatment of wastewater containing dyes. Batch adsorption tests demonstrated good adsorption capacity of hydrochars with a higher MB removal efficiency for the alkali post-treated hydrochars. Among raw hydrochars, the sample produced at 190 °C achieved the best adsorption results and, correspondingly, was characterized by a higher surface area compared to the other hydrochars. After KOH post-treatment, the sample carbonized at 250 °C showed the highest MB removal: the alkali modification contributed to a homogenization of the hydrochar surface favoring the interaction between surface functional groups and MB molecules, thus enhancing the adsorption capacity of the sample. Comparing the adsorption results with all physicochemical data from various characterization techniques, a complex mechanism for MB removal can be suggested, where surface active sites, chemical interactions and acid–base or redox equilibria between adsorbents and adsorbates can play an important role. As a whole, this work demonstrates a relatively simple process, i.e., HTC possibly followed by a cold alkali post-treatment, that allows the conversion of sewage sludge to an adsorbent material usable for water remediation.

Author Contributions: Conceptualization, R.F., L.F. and G.A.; methodology, R.F., R.C., L.F. and G.A.; validation, R.F., R.C., L.F. and G.A.; formal analysis, R.F. and V.M.; investigation, R.F., V.M., R.C.; resources, L.F., G.A., R.C.; data curation, R.F., V.M., R.C., L.F. and G.A.; writing—original draft preparation, R.F. and L.F.; writing—review and editing, R.F., L.F., R.C., G.A.; supervision, L.F.; funding acquisition, L.F. and G.A. All authors have read and agreed to the published version of the manuscript.

Funding: This research was partially funded by ECOOPERA SpA https://www.ecoopera.coop/it/.

Acknowledgments: Authors want to thank the help of some technicians of the University of Trento: Mirko D'Incau for SEM acquisition, Roberta Villa for support in the adsorption tests, Wilma Waona for ultimate analysis data. Authors want to thank also prof. Luca Fambri for TGA and Matteo Faccini for his contribution in the experimental activity.

Conflicts of Interest: The authors declare no conflict of interest.

Appendix A

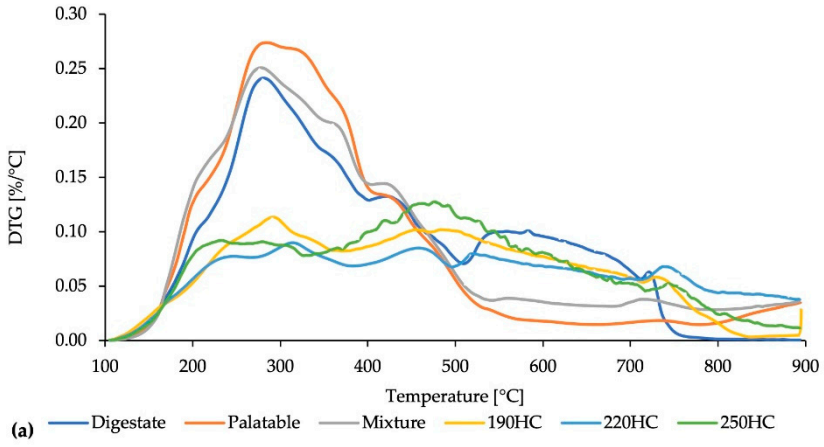

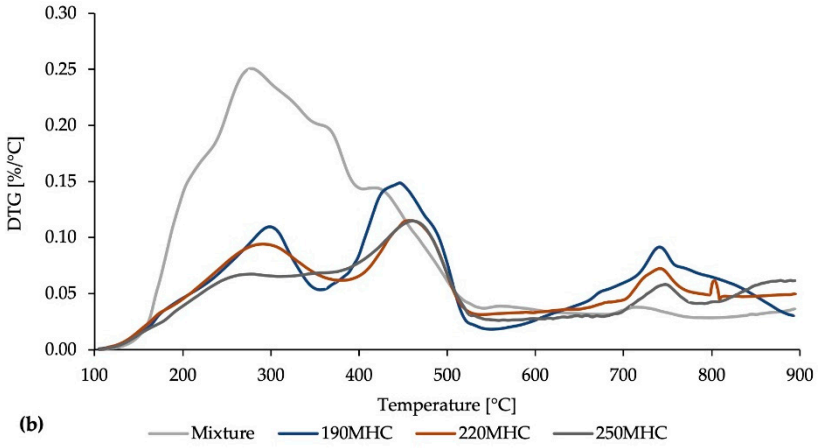

Figure A1. Derivative thermogravimetric **(**DTG) curves in N_2 atmosphere of (**a**) digestate, palatable, mixture sludge and hydrochars and (**b**) mixture sludge and modified hydrochars.

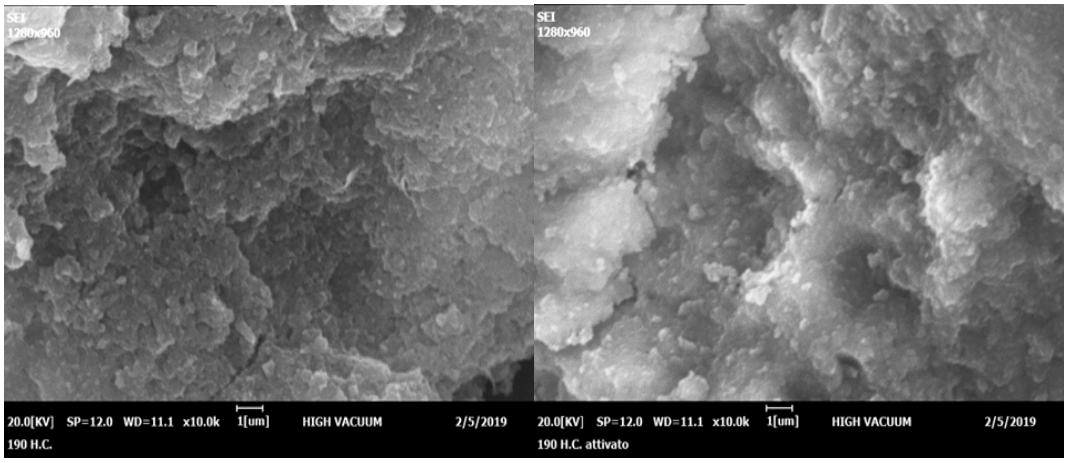

(**a**) 190HC (**b**) 190MHC

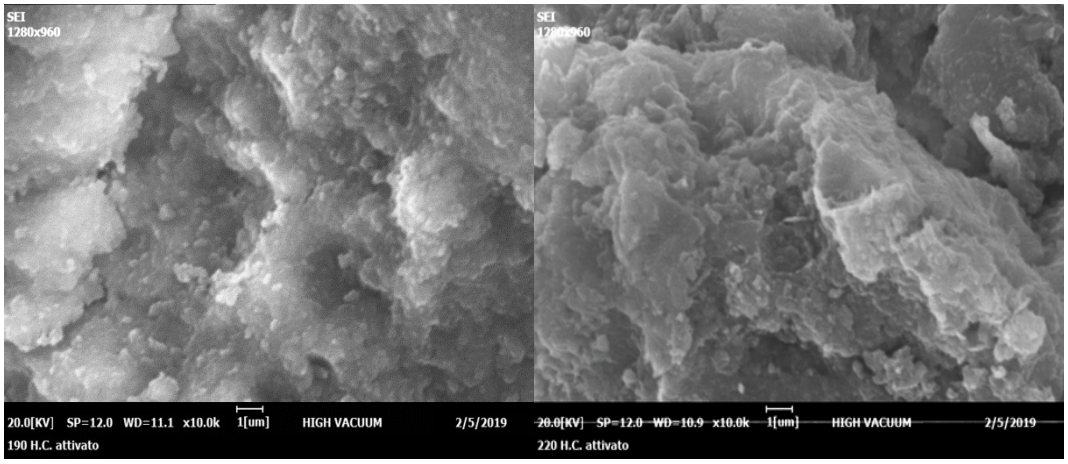

(**c**) 220HC (**d**) 220MHC

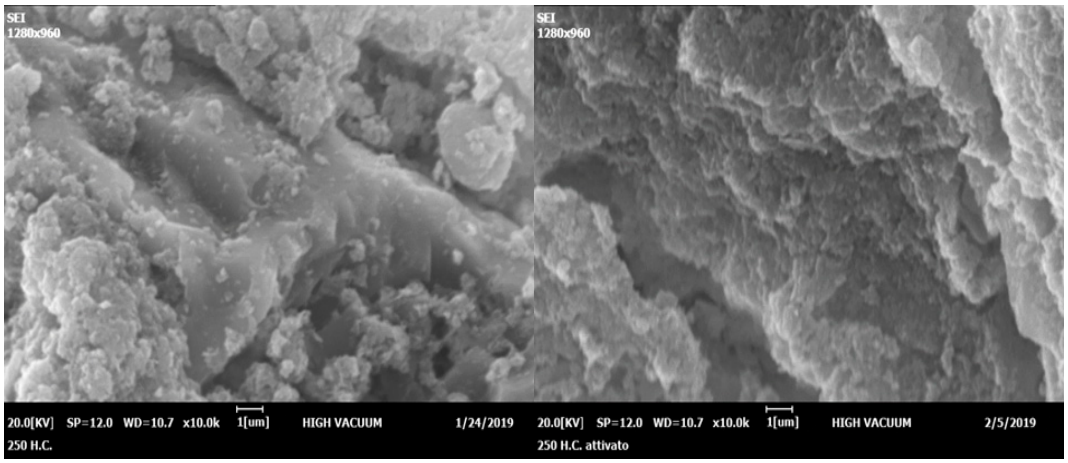

(**e**) 250HC (**f**) 250MHC

Figure A2. Scanning electron microscopy (SEM) images of (**a**) 190 °C, (**c**) 220 °C, (**e**) 250 °C raw hydrochars and (**b**) 190 °C, (**d**) 220 °C and (**f**) 250 °C modified hydrochars.

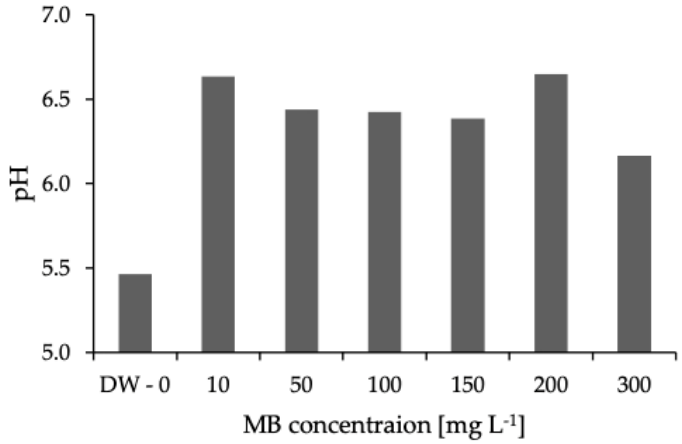

Figure A3. pH values at different MB concentrations. DW-0 represents deionized water without any MB. Standard deviation for the pH is < ±0.1.

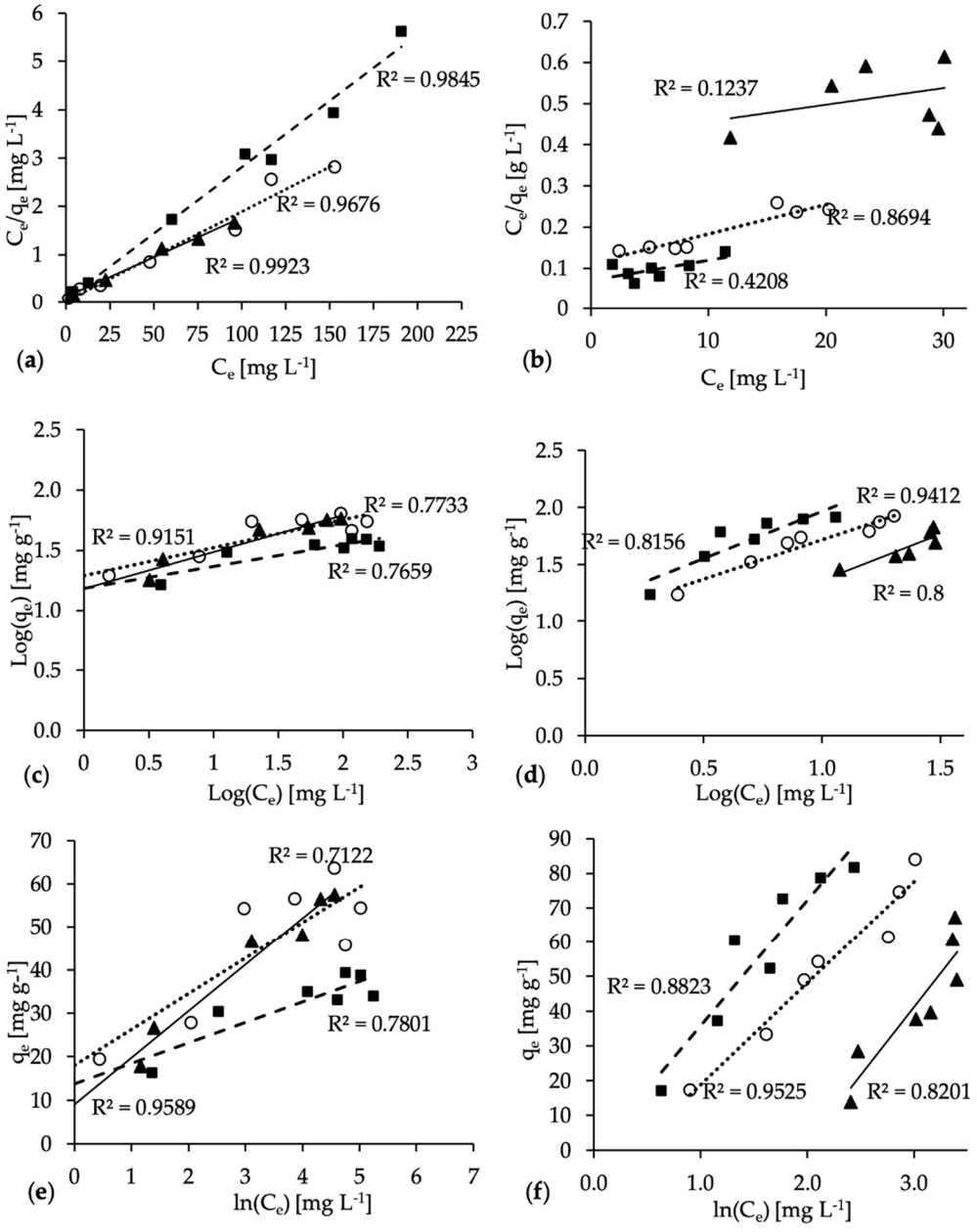

Figure A4. Linear Langmuir isotherm plots for the adsorption of MB on hydrochars (HC) (**a**) and modified hydrochars (MHC) (**b**); linear Freundlich isotherm plots for the adsorption of MB on HC (**c**) and MHC (**d**); linear Tempkin isotherm plots for the adsorption of MB on HC (**e**) and MHC (**f**) obtained at different HTC temperatures (triangle 190 °C, circle 220 °C and square 250 °C-initial MB concentrations: 10–300 mg L^{-1}; contact time: 48 h).

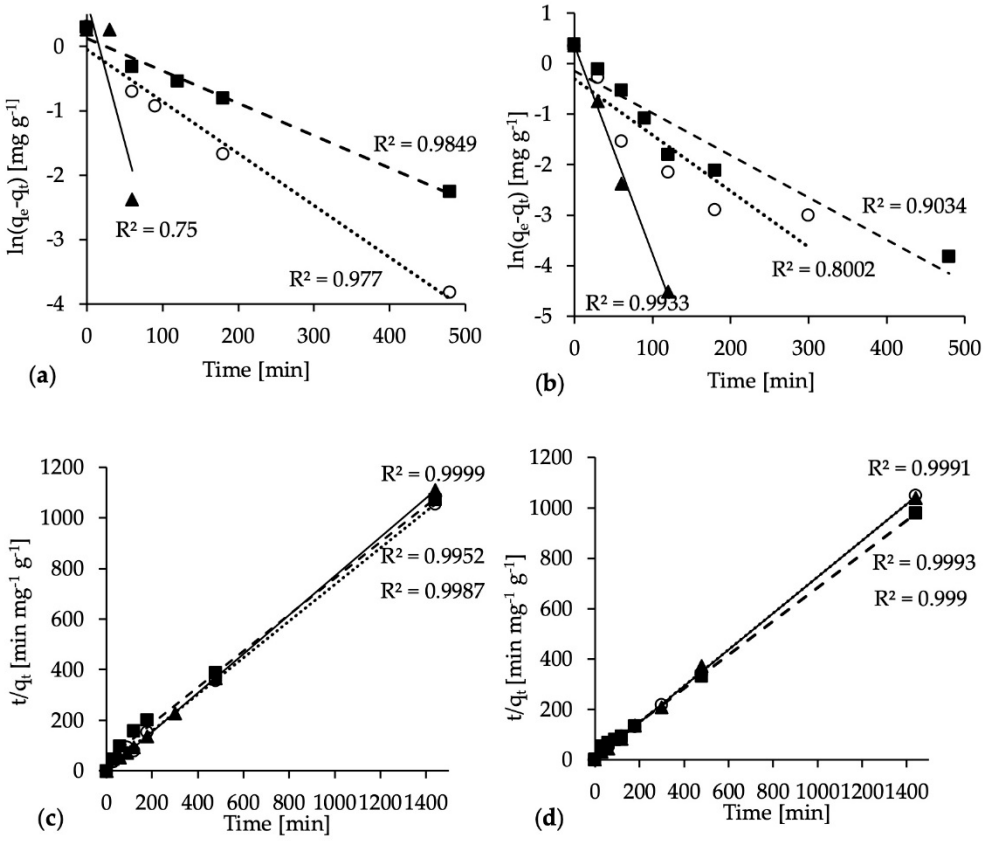

Figure A5. Pseudo first-order kinetics plots for adsorption of MB on HC (**a**) and MHC (**b**); pseudo second-order kinetics plots for adsorption of MB on HC (**c**) and MHC (**d**) (triangle 190 °C, circle 220 °C and square 250 °C-initial MB concentration: 100 mg L^{-1}; maximum contact time: 24 h).

Table A1. Content (mg kg^{-1}) of heavy metals, alkali metals and nutrients in the various samples. Absolute errors as follows: N < ±900, Al < ±800, Cd < ±0.1, Ca < ±2000, Cr < ±1, Fe < ±5000, P < ±1000, Mg < ±2000, Hg < ±0.1, Ni < ±1, Pb < ±2, K < ±700, Cu < ±10, Na < ±30, Zn < ±80.

	Digestate	Palatable	Mixture [1]	190HC	220HC	250HC	190MHC	220MHC	250MHC
N	46,400	54,300	53,200	32,800	28,000	24,700	18,800	16,000	18,500
Al	6500	6000	6000	30,000	26,600	29,400	14,200	19,900	25,800
Cd	0.9	1.0	1.0	1.6	1.4	1.5	1.5	2.1	1.6
Ca	26,000	20,000	21,000	50,000	47,000	55,000	55,000	52,000	56,000
Cr	18	19	19	28	26	33	31	27	38
Fe	27,000	24,000	24,000	50,000	45,000	51,000	50,000	47,000	52,000
P	25,000	22,000	22,000	46,000	42,000	47,000	29,000	32,000	41,000
Mg	6000	3500	4000	6000	6000	6500	7400	7300	7700
Hg	0.5	0.4	0.4	1.5	1.1	1.2	0.5	0.9	1.0
Ni	8	7.5	7.5	26	25	29	19	22	30
Pb	32	29	29	62	57	75	65	65	72
K	4900	1900	2400	1300	1000	1200	121,800	63,600	28,700
Cu	140	130	130	370	330	360	340	380	400
Na	2750	900	1170	840	610	700	1630	1210	890
Zn	490	460	470	1240	1140	1380	600	950	1160

[1] calculated as the average of the values of digestate and palatable (weighted average considering the relevant dry matter content).

Table A2. Experimental data of the isotherm adsorption batch tests for raw hydrochar (n.a.: not available).

C_0 [mg L^{-1}]	190HC				220HC				250HC			
	C_e [mg L^{-1}]	HC Mass [g]	q_e [mg g^{-1}]	MB Removal [%]	C_e [mg L^{-1}]	HC Mass [g]	q_e [mg g^{-1}]	MB Removal [%]	C_e [mg L^{-1}]	HC Mass [g]	q_e [mg g^{-1}]	MB Removal [%]
10	2	0.0150	3	80	0	0.0126	3	97	2	0.0101	3	82
50	3	0.0105	18	94	2	0.0100	19	97	4	0.0113	16	92
100	4	0.0144	27	96	8	0.0133	28	92	13	0.0115	30	87
174	22	0.0130	47	87	20	0.0114	54	89	60	0.0131	35	65
198	54	0.0119	48	73	48	0.0106	57	76	102	0.0116	33	48
239	75	0.0116	56	69	n.a.	n.a.	n.a.	n.a.	117	0.0124	39	51
279	n.a.	n.a.	n.a.	n.a.	96	0.0115	64	65	152	0.0131	39	45
295	96	0.0139	80	68	153	0.0105	54	48	191	0.0123	34	35

Table A3. Experimental data of the isotherm adsorption batch tests for modified hydrochar.

C_0 [mg L^{-1}]	190MHC				220MHC				250MHC			
	C_e [mg L^{-1}]	HC Mass [g]	q_e [mg g^{-1}]	MB Removal [%]	C_e [mg L^{-1}]	HC Mass [g]	q_e [mg g^{-1}]	MB Removal [%]	C_e [mg L^{-1}]	HC Mass [g]	q_e [mg g^{-1}]	MB Removal [%]
10	4	0.0105	2	62	2	0.0108	3	83	1	0.0107	3	88
50	11	0.0112	14	78	2	0.0110	17	95	2	0.0112	17	96
100	12	0.0124	28	88	5	0.0114	33	95	3	0.0104	37	97
144	21	0.0131	38	86	7	0.0112	49	95	5	0.0106	52	96
167	23	0.0145	40	86	8	0.0117	54	95	4	0.0108	60	98
209	30	0.0146	49	86	16	0.0126	61	92	6	0.0112	73	97
254	29	0.0148	61	89	18	0.0127	74	93	8	0.0125	79	97
295	30	0.0158	67	90	20	0.0131	84	93	11	0.0139	82	96

References

1. Ferrentino, R.; Langone, M.; Andreottola, G.; Rada, E.C. An anaerobic side-stream reactor in wastewater treatment: A review. *WIT Trans. Ecol. Environ.* **2014**, *191*, 1435–1446.
2. Saetea, P.; Tippayawong, N. Recovery of Value-Added Products from Hydrothermal Carbonization of Sewage Sludge. *ISRN Chem. Eng.* **2013**, *2013*, 1–6.
3. Sharma, H.B.; Sarmah, A.K.; Dubey, B. Hydrothermal carbonization of renewable waste biomass for solid biofuel production: A discussion on process mechanism, the influence of process parameters, environmental performance and fuel properties of hydrochar. *Renew. Sustain. Energy Rev.* **2020**, *123*, 109761.
4. Villamil, J.A.; de la Rubia, M.A.; Diaz, E.; Mohedano, A.F. *Technologies for Wastewater Sludge Utilization and Energy Production: Hydrothermal Carbonization of Lignocellulosic Biomass and Sewage Sludge*; Elsevier Inc.: Amsterdam, The Netherlands, 2020; ISBN 9780128162040.
5. Merzari, F.; Langone, M.; Andreottola, G.; Fiori, L. Methane production from process water of sewage sludge hydrothermal carbonization. A review. Valorising sludge through hydrothermal carbonization. *Crit. Rev. Environ. Sci. Technol.* **2019**, *49*, 1–42.
6. Román, S.; Libra, J.; Berge, N.; Sabio, E.; Ro, K.; Li, L.; Ledesma, B.; Alvarez, A.; Bae, S. Hydrothermal carbonization: Modeling, final properties design and applications: A review. *Energies* **2018**, *11*, 1–28.
7. Funke, A.; Ziegler, F. Hydrothermal carbonization of biomass : A summary and discussion of chemical mecha- nisms for process engineering. *Biofuels Bioprod. Biorefining* **2010**, *4*, 160–177.
8. Lucian, M.; Volpe, M.; Fiori, L. Hydrothermal Carbonization Kinetics of Lignocellulosic Agro-Wastes: Experimental Data and Modeling. *Energies* **2019**, *12*, 1–20.
9. Fang, J.; Zhan, L.; Ok, Y.S.; Gao, B. Minireview of potential applications of hydrochar derived from hydrothermal carbonization of biomass. *J. Ind. Eng. Chem.* **2018**, *57*, 15–21.
10. Román, S.; Valente Nabais, J.M.; Ledesma, B.; González, J.F.; Laginhas, C.; Titirici, M.M. Production of low-cost adsorbents with tunable surface chemistry by conjunction of hydrothermal carbonization and activation processes. *Microporous Mesoporous Mater.* **2013**, *165*, 127–133.

11. Purnomo, C.W.; Castello, D.; Fiori, L. Granular Activated Carbon from Grape Seeds Hydrothermal Char. *Appl. Sci.* **2018**, *8*, 331.
12. Hammud, H.H.; Shmait, A.; Hourani, N. Removal of Malachite Green from water using hydrothermally carbonized pine needles. *RSC Adv.* **2015**, *5*, 7909–7920.
13. Wei, J.; Liu, Y.; Li, J.; Yu, H.; Peng, Y. Removal of organic contaminant by municipal sewage sludge-derived hydrochar: Kinetics, thermodynamics and mechanisms. *Water Sci. Technol.* **2018**, *78*, 947–956.
14. Sun, K.; Tang, J.; Gong, Y.; Zhang, H. Characterization of potassium hydroxide (KOH) modified hydrochars from different feedstocks for enhanced removal of heavy metals from water. *Environ. Sci. Pollut. Res.* **2015**, *22*, 16640–16651.
15. Diaz, E.; Manzano, F.J.; Villamil, J.; Rodriguez, J.J.; Mohedano, A.F. Low-Cost Activated Grape Seed-Derived Hydrochar through Hydrothermal Carbonization and Chemical Activation for Sulfamethoxazole Adsorption. *Appl. Sci.* **2019**, *9*, 1–14.
16. Falco, C.; Marco-Lozar, J.P.; Salinas-Torres, D.; Morallón, E.; Cazorla-Amorós, D.; Titirici, M.M.; Lozano-Castelló, D. Tailoring the porosity of chemically activated hydrothermal carbons: Influence of the precursor and hydrothermal carbonization temperature. *Carbon N. Y.* **2013**, *62*, 346–355.
17. Park, J.E.; Lee, G.B.; Hong, B.U.; Hwang, S.Y. Regeneration of Activated Carbons Spent by Waste Water Treatment Using KOH Chemical Activation. *Appl. Sci.* **2019**, *9*, 1–10.
18. Regmi, P.; Garcia Moscoso, J.L.; Kumar, S.; Cao, X.; Mao, J.; Schafran, G. Removal of copper and cadmium from aqueous solution using switchgrass biochar produced via hydrothermal carbonization process. *J. Environ. Manag.* **2012**, *109*, 61–69.
19. Spataru, A.; Jain, R.; Chung, J.W.; Gerner, G.; Krebs, R.; Lens, P.N.L. Enhanced adsorption of orthophosphate and copper onto hydrochar derived from sewage sludge by KOH activation. *RSC Adv.* **2016**, *6*, 101827–101834.
20. Lucian, M.; Fiori, L. Hydrothermal carbonization of waste biomass: Process design, modeling, energy efficiency and cost analysis. *Energies* **2017**, *10*, 211.
21. Merzari, F.; Lucian, M.; Volpe, M.; Andreottola, G.; Fiori, L. Hydrothermal carbonization of biomass: Design of a bench-Scale reactor for evaluating the heat of reaction. *Chem. Eng. Trans.* **2018**, *65*, 43–48.
22. Volpe, M.; Wüst, D.; Merzari, F.; Lucian, M.; Andreottola, G.; Kruse, A.; Fiori, L. One stage olive mill waste streams valorisation via hydrothermal carbonisation. *Waste Manag.* **2018**, *80*, 224–234.
23. Sun, K.; Ro, K.; Guo, M.; Novak, J.; Mashayekhi, H.; Xing, B. Sorption of bisphenol A, 17α-ethinyl estradiol and phenanthrene on thermally and hydrothermally produced biochars. *Bioresour. Technol.* **2011**, *102*, 5757–5763.
24. Fiori, L.; Valbusa, M.; Lorenzi, D.; Fambri, L. Modeling of the devolatilization kinetics during pyrolysis of grape residues. *Bioresour. Technol.* **2012**, *103*, 389–397.
25. García, R.; Pizarro, C.; Lavín, A.G.; Bueno, J.L. Biomass proximate analysis using thermogravimetry. *Bioresour. Technol.* **2013**, *139*, 1–4.
26. CNR-IRSA. *Metodi Analitici Per i Fanghi*; CNR-IRSA: Montelibretti, Italy, 1985.
27. Guo, J.Z.; Li, B.; Liu, L.; Lv, K. Removal of methylene blue from aqueous solutions by chemically modified bamboo. *Chemosphere* **2014**, *111*, 225–231.
28. Qian, W.; Luo, X.; Wang, X.; Guo, M.; Li, B. Removal of methylene blue from aqueous solution by modi fi ed bamboo hydrochar. *Ecotoxicol. Environ. Saf.* **2018**, *157*, 300–306.
29. Langmuir, I. The constitution and fundamental properties of solids and liquids. *J. Am. Chem. Soc.* **1916**, *38*, 2221–2295.
30. Freundlich, H. Uber Die Adsorption in Losungen. *Zeitschrift fur Physikalische Chemie* **1906**, *57*, 385–470.
31. Malik, P.K. Use of activated carbons prepared from sawdust and rice-husk for adsoprtion of acid dyes: A case study of acid yellow 36. *Dye. Pigment.* **2003**, *56*, 239–249.
32. Foo, K.Y.; Hameed, B.H. Preparation, characterization and evaluation of adsorptive properties of orange peel based activated carbon via microwave induced K 2CO 3 activation. *Bioresour. Technol.* **2012**, *104*, 679–686.
33. Ho, Y.S.; Ng, J.C.Y.; McKay, G. Kinetics of pollutant sorption by biosorbents: Review. *Sep. Purif. Methods* **2000**, *29*, 189–232.
34. Ho, Y.S.; McKay, G. Pseudo-second order model for sorption processes. *Process Biochem.* **1999**, *34*, 451–465.

35. Zhai, Y.; Peng, C.; Xu, B.; Wang, T.; Li, C. Hydrothermal carbonisation of sewage sludge for char production with different waste biomass : Effects of reaction temperature and energy recycling. *Energy* **2017**, *127*, 167–174.
36. He, C.; Giannis, A.; Wang, J. Conversion of sewage sludge to clean solid fuel using hydrothermal carbonization : Hydrochar fuel characteristics and combustion behavior. *Appl. Energy* **2013**, *111*, 257–266.
37. Kang, S.; Li, X.; Fan, J.; Chang, J. Characterization of hydrochars produced by hydrothermal carbonization of lignin, cellulose, d-xylose, and wood meal. *Ind. Eng. Chem. Res.* **2012**, *51*, 9023–9031.
38. Berge, N.D.; Ro, K.S.; Mao, J.; Flora, J.R.V.; Chappell, M.A.; Bae, S. Hydrothermal carbonization of municipal waste streams. *Environ. Sci. Technol.* **2011**, *45*, 5696–5703.
39. Sing, K.S.W.; Everett, D.H.; Haul, R.A.W.; Moscou, L.; Pierotti, R.A.; Rouquérol, J.; Siemieniewska, T. Reporting physisorption data for gas/solid systems with special reference to the determination of surface area and porosity. *Pure Appl. Chem.* **1985**, *57*, 603–619.
40. Hameed, B.H.; Ahmad, A.L.; Latiff, K.N.A. Adsorption of basic dye (methylene blue) onto activated carbon prepared from rattan sawdust. *Dye. Pigment.* **2007**, *75*, 143–149.
41. El Qada, E.N.; Allen, S.J.; Walker, G.M. Adsorption of Methylene Blue onto activated carbon produced from steam activated bituminous coal: A study of equilibrium adsorption isotherm. *Chem. Eng. J.* **2006**, *124*, 103–110.
42. Ahmed, T.; Noor, W.; Faruk, O.; Bhoumick, M.C.; Uddin, M.T. Removal of methylene blue (MB) from waste water by adsorption on jackfruit leaf powder (JLP) in continuously stirred tank reactor. *J. Phys. Conf. Ser.* **2018**, *1086*.
43. Wiedner, K.; Rumpel, C.; Steiner, C.; Pozzi, A.; Maas, R.; Glaser, B. Chemical evaluation of chars produced by thermochemical conversion (gasification, pyrolysis and hydrothermal carbonization) of agro-industrial biomass on a commercial scale. *Biomass Bioenergy* **2013**, *59*, 264–278.
44. Wang, X.; Li, C.; Zhang, B.; Lin, J.; Chi, Q.; Wang, Y. Migration and risk assessment of heavy metals in sewage sludge during hydrothermal treatment combined with pyrolysis. *Bioresour. Technol.* **2016**, *221*, 560–567.
45. Huang, R.; Zhang, B.; Saad, E.M.; Ingall, E.D.; Tang, Y. Speciation evolution of zinc and copper during pyrolysis and hydrothermal carbonization treatments of sewage sludges. *Water Res.* **2018**, *132*, 260–269.
46. Xiong, J.B.; Pan, Z.Q.; Xiao, X.F.; Huang, H.J.; Lai, F.Y.; Wang, J.X.; Chen, S.W. Study on the hydrothermal carbonization of swine manure: The effect of process parameters on the yield/properties of hydrochar and process water. *J. Anal. Appl. Pyrolysis* **2019**, *144*, 104692.
47. Volpe, M.; Fiori, L. From olive waste to solid biofuel through hydrothermal carbonisation: The role of temperature and solid load on secondary char formation and hydrochar energy properties. *J. Anal. Appl. Pyrolysis* **2017**, *124*, 63–72.
48. Wang, L.; Li, A.; Chang, Y. Hydrothermal treatment coupled with mechanical expression at increased temperature for excess sludge dewatering: Heavy metals, volatile organic compounds and combustion characteristics of hydrochar. *Chem. Eng. J.* **2016**, *297*, 1–10.
49. Fu, J.; Chen, Z.; Wang, M.; Liu, S.; Zhang, J.; Zhang, J.; Han, R.; Xu, Q. Adsorption of methylene blue by a high-efficiency adsorbent (polydopamine microspheres): Kinetics, isotherm, thermodynamics and mechanism analysis. *Chem. Eng. J.* **2015**, *259*, 53–61.
50. Chen, L.; Bai, B. Equilibrium, kinetic, thermodynamic, and in situ regeneration studies about methylene blue adsorption by the raspberry-like TiO_2@yeast microspheres. *Ind. Eng. Chem. Res.* **2013**, *52*, 15568–15577.
51. Pathania, D.; Sharma, S.; Singh, P. Removal of methylene blue by adsorption onto activated carbon developed from Ficus carica bast. *Arab. J. Chem.* **2017**, *10*, S1445–S1451.